

# Effect of Carboxylation on Carbon Nanotube Aqueous Dispersibility: A Predictive Coarse-Grained Molecular Dynamics Approach

Chi-cheng Chiu,<sup>†</sup> Russell H. DeVane,<sup>‡</sup> Michael L. Klein,<sup>§</sup> Wataru Shinoda,<sup>||</sup> Preston B. Moore,<sup>⊥</sup> and Steven O. Nielsen<sup>\*,†</sup>

<sup>†</sup>Department of Chemistry, The University of Texas at Dallas, 800 West Campbell Road, Richardson, Texas 75080, United States

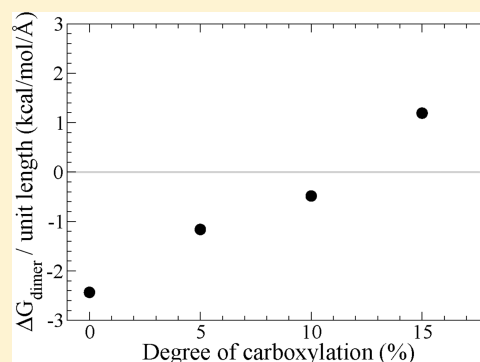
<sup>‡</sup>Corporate R&D, Modeling and Simulation, The Procter and Gamble Company, Cincinnati, Ohio 45069, United States

<sup>§</sup>Institute for Computational Molecular Science, Department of Chemistry, Temple University, 231 South 34th Street, Philadelphia, Pennsylvania 19104-6323, United States

<sup>||</sup>National Institute of Advanced Industrial Science and Technology (AIST), 1-8-31 Midorigaoka, Ikeda 563-8577, Japan

<sup>⊥</sup>Department of Chemistry & Biochemistry, University of the Sciences in Philadelphia, 600 South 43rd Street, Philadelphia, Pennsylvania 19104, United States

**ABSTRACT:** Functionalized single-walled carbon nanotubes (SWNTs) are widely applied in biomedical science. To understand the interaction between SWNTs and biological systems, various studies have attempted to use coarse-grained molecular dynamics (CGMD). However, there is limited validation of the existing CG models of SWNTs. Here, we present CG models for both pristine and carboxylated SWNTs which are validated against experimental dispersion data. In addition, we present the first ever DLVO analysis of the colloidal stability of parallel SWNTs and establish that the solvent-induced repulsion between fullerenes, which is not considered in DLVO theory, is crucial to obtain a correct physical picture of SWNT dispersibility. The results presented here provide physical insight into the colloidal stability of SWNTs and can be applied to large-scale MD studies of biological systems.



## INTRODUCTION

Single-walled carbon nanotubes (SWNTs) have drawn significant attention due to their remarkable potential in nanoelectronics, energy conservation devices, and more recently biomedicine.<sup>1–3</sup> However, the extreme hydrophobicity of SWNTs and their uncontrolled aggregation into bundles and ropes is a major obstacle for their practical use. In the comprehensive review article on the use of carbon nanotubes in biology and medicine by Liu et al., it is emphasized that SWNT surface functionalization is of critical importance.<sup>3</sup> SWNTs have to be functionalized in order to disperse them in water, render them biocompatible, and/or allow for their conjugation with additional moieties such as cell targeting agents.

One of the most popular SWNT functionalization methods is nitric acid oxidation, which introduces carboxylic and other oxygen-containing groups to the otherwise inert SWNT surface, allowing them to be dispersed in water and introducing a wealth of potential coupling points. However, this procedure also generates oxidation debris by breaking up SWNTs during oxidation or by oxidizing carbonaceous impurities present in pristine SWNT samples.<sup>4</sup> At the cost of reduced yield, Heister et al. recently showed that washing with 0.01 M NaOH removes the oxidation debris, leaving behind a functionalized SWNT sample.<sup>5</sup> With the emergence of SWNT applications, the environmental, health, and safety implications of this nanomaterial have also gained attention.<sup>2</sup>

The toxicity of fullerenes still remains controversial throughout the literature, due to the differences in toxicity assays, sources of fullerenes, and functionalization processes among other factors. Mutlu et al. study *in vivo* pulmonary toxicity in mice and conclude that 30 days after lung exposure granuloma-like structures were observed in mice treated with aggregated SWNTs. These structures were absent in mice treated with dispersed SWNTs, leading the authors to suggest that aggregation was a key toxicity factor.<sup>6</sup> Salonen et al. reached a similar conclusion in their study of phenolic acid functionalized fullerenes. The particles aggregated in response to cell membrane interactions and caused a toxic response.<sup>7</sup> Other researchers have made a link between fullerene water dispersibility (through lipid bilayer vs water partitioning) and toxicity.<sup>8,9</sup> Yet, there is only limited understanding of how fullerenes interact with living organisms. In particular, the mechanism of penetration through (or disruption of) a lipid membrane has not yet been established.

Computer simulations provide a means to gain a molecular understanding of the physical and chemical properties of nanoscale systems. Indeed, massive atomistic molecular dynamics (AAMD) simulations on petaflop supercomputers

Received: July 30, 2012

Revised: October 16, 2012

Published: October 17, 2012

are beginning to probe the machinery of life.<sup>10</sup> However, time scale limitations put most interesting phenomena out of the reach of a brute-force AAMD treatment.<sup>11</sup> To overcome this limitation, so-called coarse-grained (CG) models have been developed, in which the fundamental interaction site is a group of ~10 atoms, that allow MD to simulate mesoscale systems on the micrometer size range and millisecond time scale while retaining molecular detail.<sup>12</sup> Recent CG studies using the MARTINI force field have shed light on the biophysics of C<sub>60</sub> and SWNT interactions with lipid bilayers.<sup>9,13–15</sup> However, it has been pointed out that to use these approaches as a predictive tool the force field parameters must be validated.<sup>16</sup> Unfortunately, there are very few reports on CG models for fullerene molecules, particularly for carbon nanotubes.

Maciel et al. recommend parametrizing MD force fields against experimental transfer and solvation free energy data.<sup>17</sup> On the basis of this idea, we developed a systematic approach and used experimental and AA thermodynamic (free energy) data to reproduce key properties including surface/interfacial tension, bulk density, compressibility, hydration/transfer free energy, and distribution functions obtained from AAMD simulations. In a series of very recent studies, we developed and validated CG parameters for lipids, amino acids, and fullerenes.<sup>18–22</sup> Using this model, we studied the colloidal stability of spherical fullerenes in aqueous, hydrocarbon, and lipid bilayer environments. Here, we bring all of our studies together and extend our CG model to examine the colloidal stability of carboxylated SWNTs in an aqueous environment and compare to experimental data and to the predictions from colloid theory. Interestingly, we will see that colloid theory fails due to a well-known deficiency arising from solvation effects.<sup>23</sup>

## ■ COMPUTATIONAL METHODS

**Coarse-Grain Model.** The CG representation for a pristine SWNT was constructed with an AA/CG mapping ratio of 1.5, where each CG bead was modeled using the 4-site CG benzene (denoted BER) parameters of DeVane et al.<sup>20,21</sup> The resulting SWNT is treated as a rigid cylinder using the module provided in LAMMPS.<sup>24</sup> The CG model for water was taken from the force field developed by Shinoda et al.<sup>25</sup> Two (13,0) CG SWNTs of 12.5 Å in diameter and 31.3 Å in length were solvated with ~4900 CG water sites in a 31.3 × 120.8 × 120.8 Å<sup>3</sup> simulation box.

We then applied the approach of D’Rozario et al.<sup>9</sup> to model fullereneol by extending our CG model to carboxylated SWNTs by replacing CG BER sites with CG sites of charged amino acid side chains (ASP or GLU).<sup>18</sup> Specifically, the BER sites of a pristine SWNT were randomly replaced by charged amino acid sites, each carrying a -1 charge, to construct a carboxylated SWNT. Through tuning the amount of BER site replacement, we could generate SWNTs with different degrees of carboxylation. This procedure generates nanotubes that reflect closely what is known experimentally. For example, Yi and Chen conclude from XPS analysis that, for acid-oxidized multiwalled carbon nanotubes, dissociated carboxyl groups at pH 7.1 are the main contributor to the nanotube surface charge.<sup>26</sup> Water CG sites were randomly chosen to carry +1 charges to neutralize the negative charges on the carboxylated SWNTs. In this CG model, all the electrostatic interactions were evaluated with a dielectric constant of 80.

During the acidic functionalization, amorphous carbon impurities could also be oxidized and subsequently adsorbed to the SWNT surface acting as a kind of surfactant to disperse

SWNTs.<sup>5,27,28</sup> These amorphous carbon molecules can be removed after a treatment with base, indicating strong adsorption. In terms of our CG model we could imagine the carboxylated site (ASP) represents either direct sidewall oxidation or an oxidized amorphous carbon fragment together with a few nearby SWNT carbon atoms. In either case the CG model is consistent with the available experimental data.

All the CGMD simulations were carried out using the LAMMPS MD package from the Sandia National Laboratory.<sup>29</sup> A two-level RESPA multitime step integrator was used to calculate the equations of motion.<sup>30</sup> The bond and angle potentials were evaluated in the inner time step of 1 fs, and the nonbonded interactions were evaluated in the outer time step of 10 fs. The van der Waals and the short-range electrostatic interactions were truncated at 15 Å. To more accurately describe the electrostatic, the Coulomb interactions were evaluated by Ewald summation.<sup>31</sup> The temperature and the pressure were controlled using the Nose–Hoover algorithm at 300 K and 1 atm.<sup>32</sup>

Previously, Chiu et al. showed that the dimerization free energy between two nanoparticles can be correlated to their colloidal stability.<sup>33</sup> In addition, when SWNTs form aggregates, they tend to form bundles in which they are aligned in a parallel manner to maximize the van der Waals attraction.<sup>34,35</sup> Hence, we used the MD dimerization free energy of two parallel carboxylated SWNTs in an aqueous environment as a proxy for the SWNT colloidal stability. The CG SWNT dimerization free energy was evaluated based on Jarzynski’s equality using steered MD (SMD).<sup>36,37</sup> The reaction coordinate was chosen as the separation distance between the two SWNT long axes and ranged from 46 to 16 Å. A pulling velocity of 1 Å/ns and a force constant of 100 kcal/(mol Å<sup>2</sup>) were used for all the SMD runs. Each free energy profile was sampled with 20 SMD simulations. Simulations of inward and outward pulling give similar results, indicating the systems were at quasi-equilibrium. Using the stiff spring approximation of Park and Schulten, the free energy profile was extracted based on the first-order cumulant expansion formula, the second-order cumulant expansion formula, and the full exponential (infinite cumulant) formula.<sup>37</sup> The agreement between the free energy curves derived from the second-order cumulant and that from the full exponential formula was also used to ensure that the work distribution was Gaussian and hence that the system was in the linear response regime.<sup>37</sup> For convenience, only the full exponential results for inward pulling runs are plotted. To evaluate the effect of solvent, we performed the same dimerization free energy calculations in vacuum with the presence of counterions and a dielectric constant of 80. The electrostatic interactions were evaluated with full Ewald summation, consistent with aqueous systems.

**DLVO Theory.** The aqueous dispersibility of SWNTs is intrinsically related to their colloidal stability. Hence, it is instructive to investigate the problem from the viewpoint of the classic theory of colloidal stability pioneered by Derjaguin, Landau, Verwey, and Overbeek, known as DLVO theory. This theory considers the stability to depend on the balance between an attractive van der Waals term and a repulsive electrostatic double-layer term.

The van der Waals attraction between two colloidal bodies is typically treated at the continuum level in DLVO theory with either the Hamaker or the Lifshitz formulation.<sup>23,38</sup> Although the Lifshitz approach in principle takes into account the nature of the medium separating the colloidal bodies, even modern

treatments of hydration phenomena have generated much controversy: see Chiu et al.<sup>33</sup> for a discussion. Instead, here we simply took the direct van der Waals interaction between the two cylinders by explicit summation which is available to us from the MD simulations: for each separation distance we summed the van der Waals component of the force field over all pairs of CG beads where each pair consists of one bead on one SWNT and another bead on the other SWNT. This can be thought of as an “exact” Hamaker treatment.

The electrostatic repulsion between two parallel cylinders, with ionizable groups on their surfaces and immersed in an aqueous medium, was rigorously considered by Brenner and McQuarrie in a different context.<sup>39</sup> This theory uses a two-center expansion method to develop an analytic solution and only deviates from the classic DLVO approach in that it uses a self-consistent boundary condition so that the degree of dissociation of the ionizable groups is a function of their local environment. We used the Brenner and McQuarrie formulas, as reported, with six input parameters: the cylinder radius, the surface area per ionizable group (assumed here to be carboxylic acid), the pH, the temperature, the ionic strength, and the dielectric constant of the medium. Specifically, the input parameters consisted of a cylinder radius of 6.25 Å, a surface area per ionizable group (in Å<sup>2</sup>) of 82.1, 39.7, and 26.8 for the 5%, 10%, and 15% carboxylation levels, respectively, a pH of 7.0, a temperature of 300 K, an ionic strength (in M) of 0.055, 0.11, and 0.17 for the 5%, 10%, and 15% carboxylation levels, respectively, and a dielectric constant of 80.

## RESULTS AND DISCUSSION

To study the SWNT colloidal stability, we calculated the dimerization free energy of two parallel carboxylated SWNTs in an aqueous environment. The dimerization free energy profiles, normalized by the SWNT length, of two CG SWNTs of 12.5 Å diameter,<sup>21</sup> with 0, 5, 10, and 15% carboxylation are shown in Figure 1. The local maximum at ~19 Å corresponds to the first

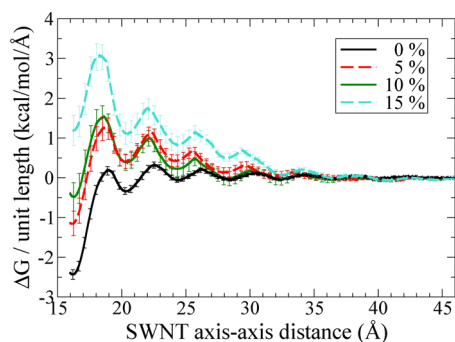


**Figure 1.** Free energy per unit length as a function of SWNT axis to axis distance for the dimerization of (13,0) CG SWNTs of 0% (black solid), 5% (red dashed), 10% (green solid), and 15% (blue dashed) carboxylation.

solvation shell around the SWNT, and the dimerization free energy at the inter-SWNT contact separation of 16.1 Å is plotted as a function of the degree of carboxylation in Figure 2. For pristine SWNTs, the dimerization free energy of  $-2.5$  kcal/(mol Å) represents a favorable dimerization free energy ( $DG_{\text{dimer}}$ ) and is in good agreement with the AA result and theoretical predictions.<sup>21,40,41</sup> Although the undulations in the free energy profile are an artifact of the CG model,<sup>21</sup> the agreement of  $DG_{\text{dimer}}$  with the AA result and theory indicates

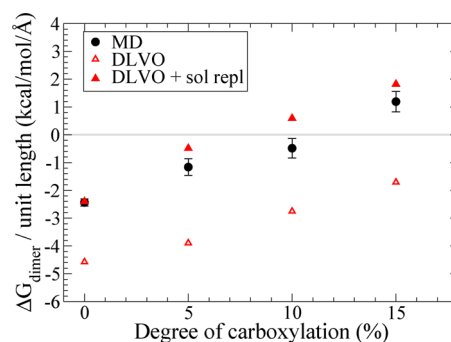


**Figure 2.** Dimerization free energy per unit length at 16.1 Å ( $DG_{\text{dimer}}$ ) plotted against the degree of SWNT carboxylation according to MD simulations (black circles), DLVO prediction (red hollow triangles), and DLVO with solvent repulsion (red solid triangles).

the correct balance between SWNT–SWNT and SWNT–water interactions of our CG model.

We found that  $DG_{\text{dimer}}$  increases monotonically with the degree of carboxylation. The crossover of  $DG_{\text{dimer}}$  from a negative to a positive value occurs between 10% and 15% carboxylation. Experimentally, the degree of functionalization of SWNTs can be controlled by, for example, the nitric acid reflux time.<sup>4,42,43</sup> Through AFM and XPS analysis, it is reported that SWNTs with more than ~12% carboxylation are mostly debundled and dispersed in aqueous solvent,<sup>43</sup> which agrees with our free energy data.

Figure 3 shows the results of the DLVO calculation compared with the MD dimerization free energy profiles in

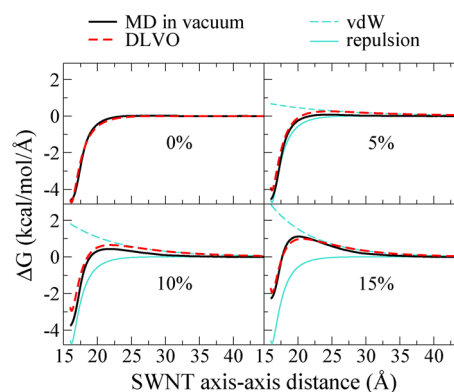


**Figure 3.** Free energy per unit length in vacuum as a function of the SWNT axis to axis distance for the dimerization of (13,0) CG SWNTs of 0%, 5%, 10%, and 15% carboxylation calculated from CGMD (black solid) compared with the predictions from DLVO theory (red dash). The DLVO data are also decomposed into the attractive van der Waals term (thin blue solid line) and the repulsive electrostatic term (thin blue dashed line).

vacuum with a dielectric constant of 80 for various carboxylated SWNTs. For all four carboxylated SWNTs systems, the DLVO predictions agree with the dimerization free energies in vacuum but differ from that in aqueous solvent (Figure 1). In DLVO theory, the separate contributions from the van der Waals (vdW) attractive term and the repulsive electrostatic term are also plotted in Figure 3. For the pristine SWNT system, since no ions are presented, only the vdW term contributes, and the resulting DLVO energy is essentially the dimerization free energy in vacuum. In fact, the vdW terms are very similar for all the carboxylated SWNT systems tested. Hence, the variations

in the DLVO energy profiles for different carboxylated SWNT systems are mainly due to the electrostatic term. In our CG model, water interaction sites do not carry charge nor provide screening; instead, we use a dielectric constant of 80. The qualitative agreement between DLVO predictions and vacuum systems shown in Figure 3 suggests that, at the nanoscale, our CG model can successfully describe the screened electrostatic repulsion as predicted by DLVO theory by adjusting the dielectric constant (80 in this study). However, DLVO theory completely misses the effect of solvation and leads to the discrepancies from the free energy profiles shown in Figure 1. Indeed, Li et al. used AAMD to demonstrate that fullerenes have an anomalously strong dispersion interaction with water, resulting in a repulsive solvent-induced contribution to the fullerene dimerization free energy,<sup>44–46</sup> which we also noted in our previous CG study.<sup>21</sup>

While DLVO theory uses an implicit solvent treatment, water molecules are explicitly modeled in our CG simulations. To quantify the solvent contribution, we subtracted the dimerization free energy profile in vacuum (but using a dielectric constant of 80) from that obtained in water for all types of SWNTs as illustrated in Figure 4. For pristine SWNTs, the

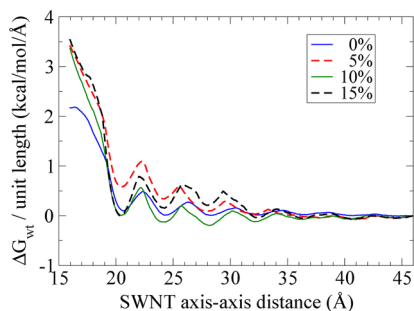


**Figure 4.** Water-induced contribution to the dimerization free energy profile for CG SWNTs of 0% (blue solid), 5% (red dashed), 10% (green solid), and 15% (black dashed) carboxylation.

repulsive interaction induced by water agrees with the result reported by Li et al.<sup>46</sup> In the range of dewetting (16–19 Å), the water-induced interaction of carboxylated SWNTs is much higher than for pristine SWNTs, indicating a stronger interaction between the carboxylated SWNTs and water. For all three carboxylated SWNT systems, the solvent has very similar contributions to the overall dimerization free energy. Combining the solvent effect and the result shown in Figure 3, it is clear that the  $DG_{\text{dimer}}$  change seen in Figures 1 and 2 is mainly due to the stronger electrostatic repulsion between two carboxylated SWNTs as described in DLVO theory. If we add the solvent contribution at 16.1 Å to the DLVO prediction, the resulting  $DG_{\text{dimer}}$  versus degree of carboxylation is comparable with the CGMD data as shown in Figure 2.

## CONCLUSIONS

In conclusion, we combined our previous CG models for SWNTs and charged amino acids to generate a CG model for carboxylated SWNTs. The model successfully describes the aqueous dispersibility of carboxylated SWNTs in comparison to experimental data. By comparing with the DLVO theory of colloidal stability we showed that (1) electrostatic double-layer repulsion plays a dominant role for carboxylated SWNTs dispersion and (2) the screened electrostatic repulsion as predicted by DLVO theory can be successfully described in our

CG model by adjusting the dielectric constant. Furthermore, we showed that a repulsive solvent-induced interaction must be included to capture the correct physics. The results presented here not only give insight into the colloidal behavior of SWNTs but also provide a foundation for future large scale CG studies of functionalized SWNTs interacting with biological systems.

## AUTHOR INFORMATION

### Corresponding Author

\*E-mail: steven.nielsen@utdallas.edu.

### Notes

The authors declare no competing financial interest.

## ACKNOWLEDGMENTS

We thank Inga H. Musselman and Pooja Bajaj for valuable discussions regarding their experimental data on SWNT carboxylation. S.O.N. acknowledges support from the SRC/SEMATECH Engineering Research Center for Environmentally Benign Semiconductor Manufacturing.

## REFERENCES

- Baughman, R. H.; Zakhidov, A. A.; de Heer, W. A. *Science* **2002**, *297*, 787–792.
- Buzea, C.; Pacheco, I. I.; Robbie, K. *Biointerphases* **2007**, *2*, MR17–MR71.
- Liu, Z.; Tabakman, S.; Welsher, K.; Dai, H. J. *Nano Res.* **2009**, *2*, 85–120.
- Hu, H.; Zhao, B.; Itkis, M. E.; Haddon, R. C. *J. Phys. Chem. B* **2003**, *107*, 13838–13842.
- Heister, E.; Lamprecht, C.; Neves, V.; Tilmaciu, C.; Datas, L.; Flahaut, E.; Soula, B.; Hinterdorfer, P.; Coley, H. M.; Silva, S. R. P.; et al. *ACS Nano* **2010**, *4*, 2615–2626.
- Mutlu, G. M.; Budinger, G. R. S.; Green, A. A.; Urich, D.; Soberanes, S.; Chiarella, S. E.; Alheid, G. F.; McCrimmon, D. R.; Szeifer, I.; Hersam, M. C. *Nano Lett.* **2010**, *10*, 1664–1670.
- Salonen, E.; Lin, S.; Reid, M. L.; Allegood, M.; Wang, X.; Rao, A. M.; Vattulainen, I.; Ke, P. C. *Small* **2008**, *4*, 1986–1992.
- Sayes, C. M.; Fortner, J. D.; Guo, W.; Lyon, D.; Boyd, A. M.; Ausman, K. D.; Tao, Y. J.; Sitharaman, B.; Wilson, L. J.; Hughes, J. B.; et al. *Nano Lett.* **2004**, *4*, 1881–1887.
- D’Rozario, R. S. G.; Wee, C. L.; Wallace, E. J.; Sansom, M. S. P. *Nanotechnology* **2009**, *20*, 115102.
- Miao, L.; Schulten, K. *Biophys. J.* **2010**, *98*, 1658–1667.
- Klein, M. L.; Shinoda, W. *Science* **2008**, *321*, 798–800.
- Nielsen, S. O.; Lopez, C. F.; Srinivas, G.; Klein, M. L. *J. Phys.: Condens. Matter* **2004**, *16*, R481–R512.
- Wong-Ekkabut, J.; Baoukina, S.; Triampo, W.; Tang, I. M.; Tieleman, D. P.; Monticelli, L. *Nat. Nanotechnol.* **2008**, *3*, 363–368.
- Wallace, E. J.; Sansom, M. S. P. *Nano Lett.* **2008**, *8*, 2751–2756.
- Shi, X. H.; Kong, Y.; Gao, H. J. *Acta Mech. Sin.* **2008**, *24*, 161–169.
- Monticelli, L.; Salonen, E.; Ke, P. C.; Vattulainen, I. *Soft Matter* **2009**, *5*, 4433–4445.
- Maciel, C.; Fileti, E. E.; Rivelino, R. *J. Phys. Chem. B* **2009**, *113*, 7045–7048.
- DeVane, R.; Shinoda, W.; Moore, P. B.; Klein, M. L. *J. Chem. Theory Comput.* **2009**, *5*, 2115–2124.
- Shinoda, W.; DeVane, R.; Klein, M. L. *J. Phys. Chem. B* **2010**, *114*, 6836–6849.
- DeVane, R.; Klein, M. L.; Chiu, C.-c.; Nielsen, S. O.; Shinoda, W.; Moore, P. B. *J. Phys. Chem. B* **2010**, *114*, 6386–6393.
- Chiu, C.-c.; DeVane, R.; Klein, M. L.; Shinoda, W.; Moore, P. B.; Nielsen, S. O. *J. Phys. Chem. B* **2010**, *114*, 6394–6400.
- DeVane, R.; Jusufi, A.; Shinoda, W.; Chiu, C.-c.; Nielsen, S. O.; Moore, P. B.; Klein, M. L. *J. Phys. Chem. B* **2010**, *114*, 16364–16372.

- (23) Liang, Y.; Hilal, N.; Langston, P.; Starov, V. *Adv. Colloid Interface Sci.* **2007**, *134–35*, 151–166.
- (24) Zhang, Z. L.; Glotzer, S. C. *Nano Lett.* **2004**, *4*, 1407–1413.
- (25) Shinoda, W.; Devane, R.; Klein, M. L. *Mol. Simul.* **2007**, *33*, 27–36.
- (26) Yi, P.; Chen, K. L. *Langmuir* **2011**, *27*, 3588–3599.
- (27) Salzmann, C. G.; Llewellyn, S. A.; Tobias, G.; Ward, M. A. H.; Huh, Y.; Green, M. L. H. *Adv. Mater.* **2007**, *19*, 883–887.
- (28) Worsley, K. A.; Kalinina, I.; Bekyarova, E.; Haddon, R. C. *J. Am. Chem. Soc.* **2009**, *131*, 18153–18158.
- (29) Plimpton, S. J. *Comput. Phys.* **1995**, *117*, 1–19.
- (30) Tuckerman, M.; Berne, B. J.; Martyna, G. J. *J. Chem. Phys.* **1992**, *97*, 1990–2001.
- (31) Allen, M. P.; Tildesley, D. J. *Computer Simulations of Liquids*; University Press: Oxford, 1992.
- (32) Hoover, W. G. *Phys. Rev. A* **1985**, *31*, 1695–1697.
- (33) Chiu, C.-c.; Moore, P. B.; Shinoda, W.; Nielsen, S. O. *J. Chem. Phys.* **2009**, *131*, 244706.
- (34) Thess, A.; Lee, R.; Nikolaev, P.; Dai, H. J.; Petit, P.; Robert, J.; Xu, C. H.; Lee, Y. H.; Kim, S. G.; Rinzler, A. G.; et al. *Science* **1996**, *273*, 483–487.
- (35) Grossiord, N.; Regev, O.; Loos, J.; Meuldijk, J.; Koning, C. E. *Anal. Chem.* **2005**, *77*, 5135–5139.
- (36) Jarzynski, C. *Phys. Rev. Lett.* **1997**, *78*, 2690–2693.
- (37) Park, S.; Khalili-Araghi, F.; Tajkhorshid, E.; Schulten, K. *J. Chem. Phys.* **2003**, *119*, 3559–3566.
- (38) Brenner, S. L.; Mcquarrie, D. A. *Biophys. J.* **1973**, *13*, 301–331.
- (39) Brenner, S. L.; Mcquarrie, D. A. *J. Colloid Interface Sci.* **1973**, *44*, 298–317.
- (40) Lum, K.; Chandler, D.; Weeks, J. D. *J. Phys. Chem. B* **1999**, *103*, 4570–4577.
- (41) Walther, J. H.; Jaffe, R. L.; Kotsalis, E. M.; Werder, T.; Halicioglu, T.; Koumoutsakos, P. *Carbon* **2004**, *42*, 1185–1194.
- (42) Zhang, M.; Yudasaka, M.; Iijima, S. *J. Phys. Chem. B* **2004**, *108*, 149–153.
- (43) Bajaj, P. Temporal Study of Single-Walled Carbon Nanotube Carboxylation by Nitric Acid Reflux. M.Sc. Thesis, The University of Texas at Dallas, Richardson, TX, 2008.
- (44) Li, L. W.; Bedrov, D.; Smith, G. D. *J. Chem. Phys.* **2005**, *123*, 204504.
- (45) Li, L. W.; Bedrov, D.; Smith, G. D. *Phys. Rev. E* **2005**, *71*, 011502.
- (46) Li, L. W.; Bedrov, D.; Smith, G. D. *J. Phys. Chem. B* **2006**, *110*, 10509–10513.